

Hydrothermal Synthesis of Sb_6O_{13} Nanocrystals and Their Properties

Elham Ghavidel Aghdam, Sanam Chamani Gouravan

Department of chemical, Ilkhchi Branch, Islamic Azad University, Ilkhchi, Iran

Received: June 10 2013

Accepted: July 10 2013

ABSTRACT

Antimony oxide with defect pyrochlore structure (Sb_6O_{13}) crystallize in the cubic system with space group Fd_3m . Antimony oxide often promotes the activating catalysts used for selective partial oxidations and for related reactions such as oxidative coupling. Antimony oxide can be used as a catalyst, retardant, fining agent and optical material. A simple hydrothermal method has been developed for synthesizing of Sb_6O_{13} nanocrystals at a high yield at $180^\circ C$ that is a new method for preparing these nanocrystals. Thoroughly mixtures of antimony oxide (Sb_2O_3) and cerium oxide (CeO_2) used as a starting material. Antimony oxide to cerium oxide molar ratio in different experiments were either 1:1, 1:2, 1:3 and, 1:4. Cell parameters were determined by CELEREF software (10.2963, 10.2951, 10.2920, 10.2997 for 1:1, 1:2, 1:3, 1:4, ratios respectively). In the all of ratios, XRD result was similar. FT-IR, XRD, UV, Fluorescence and SEM were used to analysis the structure characteristics of Sb_6O_{13} nanocrystals. Band gap for Sb_6O_{13} nano crystals is 2eV. The diameter of crystals is around 60-80 nm from SEM.

KEYWORDS: Antimony oxide; Nano crystal; Hydrothermal; Optical properties;

1. INTRODUCTION

Nanocrystalline materials have attracted considerable attention due to their distinguished electrical, optical, optoelectronic, electronic and magnetic properties [1]. Investigations on semiconductor nanostructures have recently been in the focus of intensive research activities because of intrinsic fundamental interest and manifold possibilities for applications.

Antimony oxide with defect pyrochlore structure (Sb_6O_{13}) crystallize in the cubic system with space group Fd_3m . Antimony oxide often promotes the activating catalysts used for selective partial oxidations and for related reactions such as oxidative coupling. Antimony oxide can be used as a catalyst, retardant, fining agent and optical material. Recently antimony oxide was found to have high proton conductivity, which is likely to be a promising humidity-sensing material [2-5].

The structure of Sb_6O_{13} ($Sb_2^{+3}O_3 \cdot 2 Sb_2^{+3}O_5$) can be regarded as the two cationic sub lattices belonging to the first two compounds, brought together to form one anionic framework, with random distribution of the eight Sb^{+3} cations in the (32e) position. The formula of the oxide Sb_6O_{13} ($Sb_2^{+3}Sb_4^{+5}O_{13}$) can be represented in the form $Sb^{+3}Sb_2^{+5}O_6O_{1.5}$, in accordance with the pyrochlore structure AB_2O_6X [6-7].

As a method for preparing high-quality ceramic powders, the hydrothermal synthetic route has advantages for obtaining highly-crystallized powders. Hydrothermal synthesis has been successful for the preparation of important solids such as microporous crystals, super ionic conductors, chemical sensors, electronically conducting solids, complex oxide ceramics and magnetic materials, and luminescence materials [8-11]. In this study we have established a simple technique to prepare Sb_6O_{13} pyrochlore nanocrystals by a low temperature hydrothermal method. Cerium oxide act as a auxiliary function and catalytic factor, and Sb_2O_3 in the presence of CeO_2 can undergo transformation to Sb_6O_{13} .

2. Experimental

2.1. Synthesis of Sb_6O_{13} nanocrystals

Thoroughly mixtures of antimony oxide (Sb_2O_3) and cerium nitrate ($Ce(NO_3)_3 \cdot 6H_2O$) used as a starting materials. In a typical procedure, Sb_2O_3 (0.291g) and $Ce(NO_3)_3 \cdot 6H_2O$ (0.434g) were dissolved into 10 ml of distilled water at room temperature in beaker and magnetically stirred to obtaining homogeneous solution. The as-obtained product was transferred into a Teflon lined stainless autoclave. The autoclave was sealed and maintained at $180^\circ C$ for 48h, allowed to cool naturally to room temperature. A white precipitate was collected. The product was washed and filtered several times with distilled water, and dried in room temperature.

To study molarities effect of the cerium oxide to final product, the experiment was carried out for various cerium oxide concentration and Sb_2O_3 to CeO_2 molar ratios in different experiments were either 1:1, 1:2, 1:3, 1:4. In order to study the time effect to optical properties the experiment was carried out in different times (24h, 48h).

2.2. Characterization

Powder X-ray diffraction (P-XRD) was performed with a Siemens D5000 X-ray diffractometer with Cu-K α radiation ($\lambda = 1.541 \text{ \AA}$) and 2θ was varied 4-70 $^\circ$.

The Fourier Transformed Infrared (FTIR) transmissions in the region 400-4000 cm^{-1} were recorded using the FTIR Nexus 670 by KBr pellet technique.

The morphology of the particles was examined by a scanning electron microscope (SEM, philips XLC). UV-Vis spectra data were collected over the spectral range 190 -1100 nm with a double beam UV-1700 Pharma Spec, SHIMADZU scanning double-beam spectrometer. Samples were dispersed in deionized water for 10 min under ultra sonic radiation. Florescence measurements were carried out by a perkin-elmer LS55 florescence spectrophotometer.

3. Result and Discussion

The XRD patterns of the synthesized Sb_6O_{13} were indexed to a cubic phase and Fd_3m space group with lattice parameters of $a=10.2963 \text{ \AA}$ that undertaken with celeref software. The intensity and position of the peaks are in good agreement with the values reported in the literature (JCPDS-33-011).

The molar ratio of Antimony oxide to cerium oxide in different experiments were either 1:1, 1:2, 1:3 and, 1:4. The powder XRD patterns (P-XRD) of all products are similar indicating a single phase cubic structure as Sb_6O_{13} (see fig1).

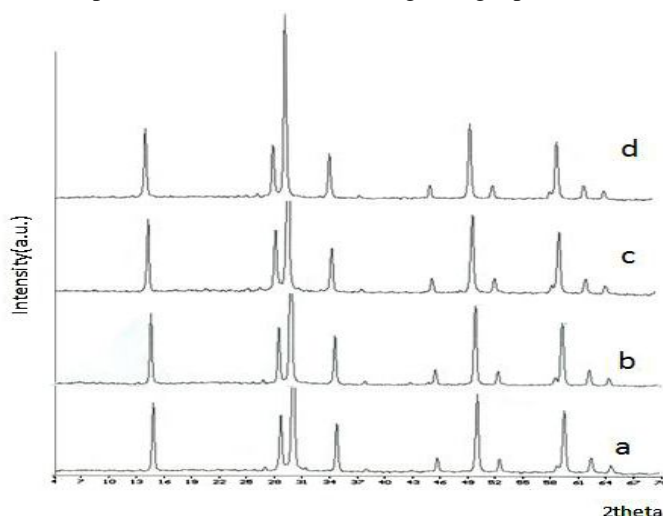


fig1

ICP measurements show no Cerium content in the products. Also the EDX measurements confirm these result (fig2).

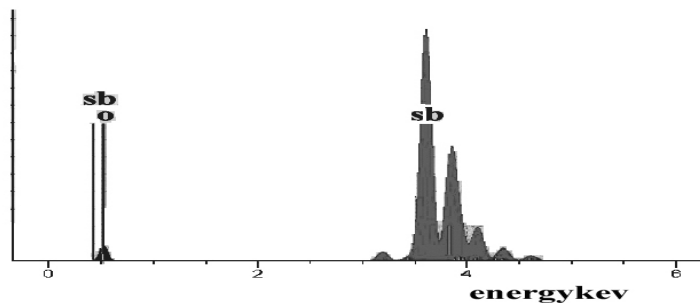


fig2

Cerium oxide acts as a auxiliary function and catalytic factor, and Sb_2O_3 in the presence of CeO_2 can undergo transformation to Sb_6O_{13} .

Cell parameters of Sb_6O_{13} nanocrystals calculated from the XRD patterns, showing that with increasing Cerium concentration the a parameter decrease until 1:3 ratio, but in 1:4 ratio it increases (fig3)

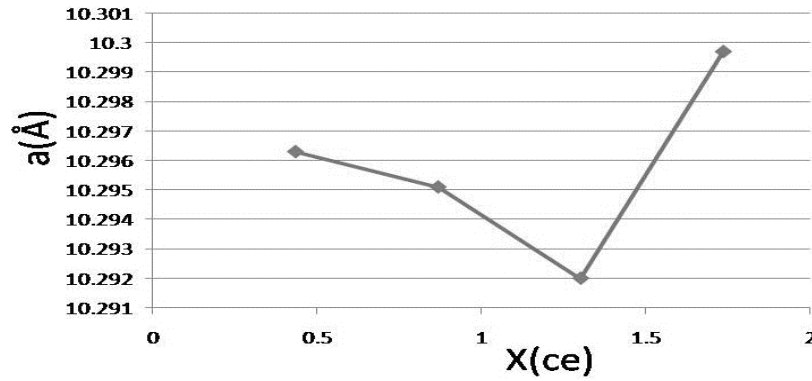


fig3

The crystal size (CS) is calculated from X-ray diffraction patterns using Scherrer's formula ($CS = K\lambda/\beta \cos \theta$, where β is the full width at the half maximum of peak corrected for instrumental broadening, λ is the wavelength of the X-ray and K is Scherrer's constant) [13]. The grain size was 70 nm. The morphology of the prepared Sb_6O_{13} was examined by SEM images indicating nanocrystals in 60-80 nm as diameter fig 4.

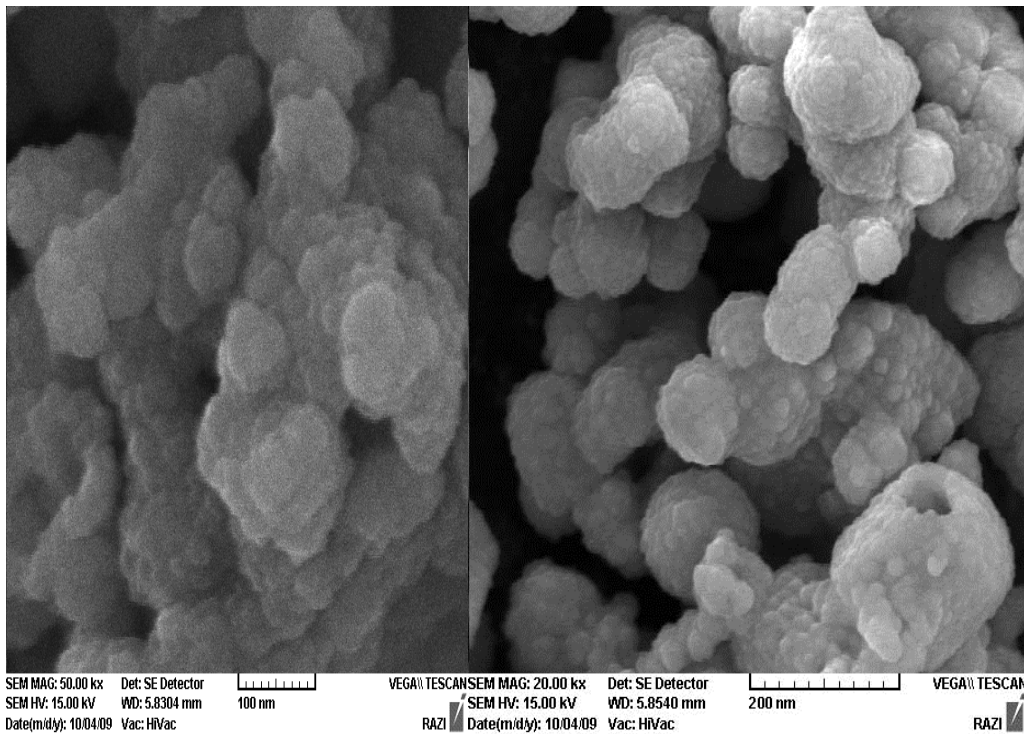


fig 4

Fig 5 Shows IR spectrum of the as obtained sample at optimized condition. Strong adsorption peaks at $459.61, 737.47 \text{ cm}^{-1}$ are correspond to the vibration of Sb -O bond in the Sb_6O_{13} lattice [14]. The bond at 1657 cm^{-1} corresponds to the deformation vibration of water molecule. it is significant that there is a small signature at 1382 cm^{-1} indicative of the presence of nitrates.

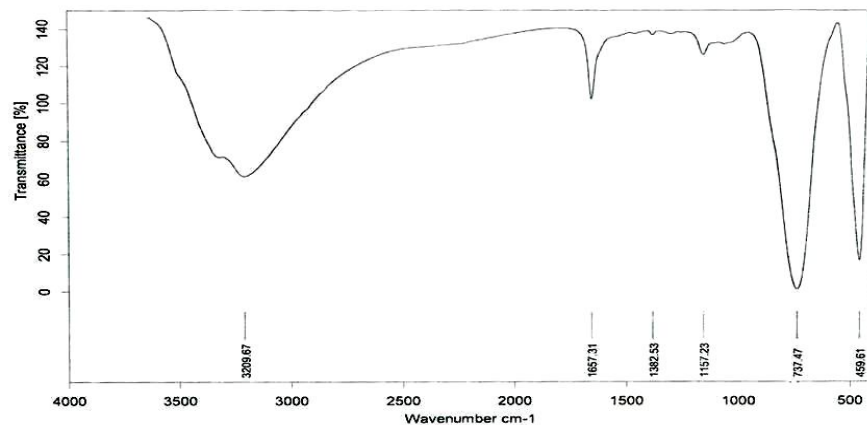


Fig 5

To study time effect on optical properties, the experiment was carried out in different times (24h, 48h). Optical absorption spectra of these samples are shown in fig 6.a,b,c. The Sb_6O_{13} prepared in 24h shows high quantum yield than Sb_6O_{13} prepared in 48h.

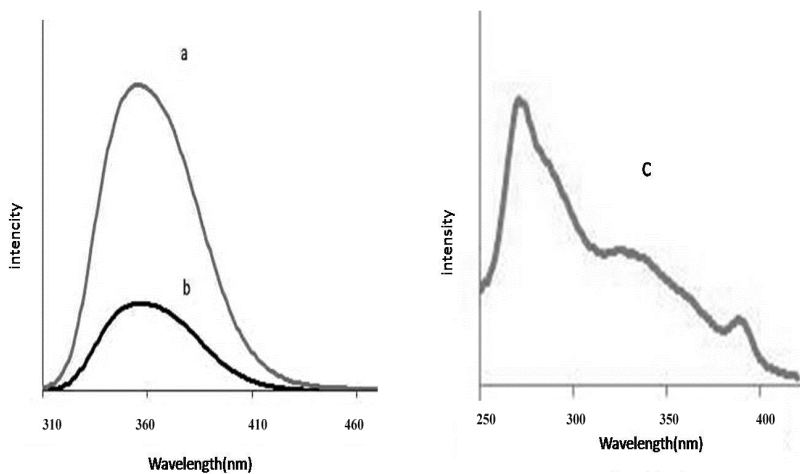


fig 6.a,b,c

The UV/Vis spectrum shows an intense absorption at 201.5 nm, probably attributed to charge transfer from $o \rightarrow sb$ and weak peak in the range of 400-650 nm (fig7). Band gap for Sb_6O_{13} (prepared in 24h) is 2eV and for Sb_6O_{13} (prepared in 48h) is 2.1 eV. Therefore, increasing reaction time leads to a decrease in the band gap of Sb_6O_{13} . Generally, the spectra of all our samples show a blue shift with increasing reaction time. This phenomenon is commonly observed for nanomaterials [15].

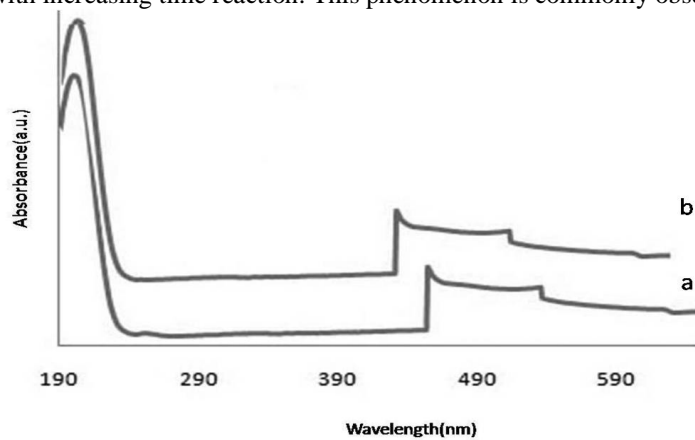


fig7

REFERENCES

- [1] F. Tao, Z. Wang, L. Yao, W. Cai, X. Li, (2007) : *J. Phys. Chem.* 111,3241.
- [2] S. Slaw, E. Golunski (1989): . A guide to phase changes during catalyst preparation, *J. Appl Catal*, 48,123-135.
- [3] T. Inoue, S. Oyama (2000): . Characterization and selective oxidation catalysis of modified Pt particles on SbO_x , *J. Appl Catal*, 191,131-140.
- [4] M. A. Surbmanian, G. Aravamudan, G. V. Subbarao (1983): Oxide pyrochlore-Review. *Prog, J. Solide st. chem.* 15,55-143.
- [5] G. Centi, T. Trifiro, (1986) : *Catal. Rew. Sci. Eng.*, 28,105.
- [6] P. Kova, L. Plyasova (1979): *Appl Catal*, 19,1040.
- [7] V. Molodtsova, D. Tarasova, A. Shkarin, (1972): *Kinet. Katal*, 13
- [8] A. Alemi, M. Dolatyari, *Radiat. Eff. Defect S.* 163(2008) 135.
- [9] E. H. Amanda B. Chris, K. S. Amandeep, D. J. Raiman, E. S. Raymond, (2006): *Chem. Mater* 18,567.
- [10] L. Kun-Wei, L. Huiling, Z. Huiming, (2006): *Mater. Res. Bull.* 41,191.
- [11] H. C. Gupta, S. Brown, N. Ranibi, V. B. Gohef, (2002) : *J. Phys. Chem* 63,535.
- [12] W. Epitaxy, L. Suchanek (2004): *Chem. Mater.*, 16,1083.
- [13] N. Benramdane, M. Latreche, H. Tabet, (1999) : *Mat. Sci. Eng.* 84,64.
- [14] C. A. Cody, L. Dicarloi, R. Darlington, (1979) : Vibrational and thermal study of antimony oxides. *Inorganic Chemistry, J. Inorg. Chem.* 18,1572-1576.
- [15] Y. Li, H. Liao, Y. Ding, (1999): *Inorg. Chem.* 38, 1382.